

Moderately Supervised Learning: Definition, Framework and Generality

Yongquan Yang^a (remy_yang@foxmail.com)

^a Laboratory of Pathology, West China Hospital, Sichuan University, 37 Guo Xue Road, 610041
Chengdu, China

Abstract

Learning with supervision has achieved remarkable success in numerous artificial intelligence (AI) applications. In the current literature, by referring to the properties of the labels prepared for the training data set, learning with supervision is categorized as supervised learning (SL) and weakly supervised learning (WSL). SL concerns the situation where the training data set is assigned with ideal (complete, exact and accurate) labels, while WSL concerns the situation where the training data set is assigned with non-ideal (incomplete, inexact or inaccurate) labels. However, solutions for various SL tasks have shown that the given labels are not always learnable and the transformation from the given labels to learnable targets can significantly affect the performance of the final SL solutions. Without considering the properties of the transformation from the given labels to learnable targets, the definition of SL is relatively abstract, which conceals some details that can be critical to building the appropriate solutions for specific SL tasks. Thus, for engineers in the AI application field, it is desirable to reveal these details more concretely. This article attempts to achieve this goal by expanding the categorization of SL and investigating the sub-type that plays the central role in SL. More specifically, taking into consideration the properties of the transformation from the given labels to learnable targets, we firstly categorize SL into three narrower sub-types. Then we focus on the moderately supervised learning (MSL) sub-type that concerns the situation where the given labels are ideal, but due to the simplicity in annotation, careful designs are required to transform the given labels into learnable targets. From the perspectives of the definition, framework and generality, we comprehensively illustrate MSL and reveal what details are concealed by the abstractness of the definition of SL. At the meantime, the whole presentation of this paper as well establishes a tutorial for AI application engineers to refer to viewing a problem to be solved from the mathematicians' vision.

1. Introduction

With the development of fundamental machine learning techniques, especially deep learning [1], learning with supervision has achieved great success in various classification and regression tasks for artificial intelligence (AI) applications. Typically, a predictive machine learning model is learned from a training dataset that contains a number of training examples. For learning with supervision, the training examples usually consist of certain training events/entities and their corresponding labels. In classification, the labels indicate the classes corresponding to the associated training events/entities; in regression, the labels are real-value responses corresponding to the associated training events/entities.

In the current literature of learning with supervision, there are two main streams: supervised learning (SL) and weakly supervised learning (WSL) [2]. SL focuses on the situation where the training events/entities are assigned with ideal labels. The word ‘ideal’ here refers to that the labels assigned to the training events/entities are complete, exact and accurate. ‘Complete’ indicates that each training event/entity is assigned with a label. ‘Exact’ indicates that the label of each training event/entity is individually assigned. ‘Accurate’ indicates that the assigned label can accurately describe the ground-truth of the corresponding event/entity. In contrast, WSL focuses on the situation where the training events/entities are assigned with non-ideal labels. The word non-ideal here refers to that the labels assigned to the training events/entities are incomplete, inexact or inaccurate. ‘Incomplete’ indicates that, only a proportion of training events/entities are assigned with labels. ‘Inexact’ indicates that several training events/entities can be simultaneously assigned with a same label. ‘Inaccurate’ indicates that the assigned label cannot accurately describe the ground-truth of the corresponding event/entity. More formal descriptions for the definitions of SL and WSL are provided in Section 2.

The clear boundary between the definitions of SL and WSL is the properties (completeness, exactness and accuracy) of the labels prepared for the training events/entities. However, in many real-world practice of SL tasks, we cannot directly learn a predictive model that can effectively map the training events/entities to their correspondingly assigned labels. The main reason lies in the fact that the assigned labels are not always learnable, though ideal (complete, exact and accurate) are they. We must first transform the assigned labels into learnable targets for learning the predictive model of a SL solution. Existing solutions for various SL tasks have shown that the transformation from the given labels to the learnable targets can significantly affect the performance of the final SL solution [3–7]. By simply referring to the properties (completeness, exactness and accuracy) of the labels prepared for the training events/entities, the definition of SL is relatively abstract. Without considering the properties of the transformation from the given labels to the learnable targets, the abstractness of the definition of SL conceals some details that can be critical to building the appropriate solutions for certain specific SL tasks. Thus, for practitioners in the application field of SL, it is desirable to reveal these details more concretely. This article attempts to achieve this goal by expanding the categorization of SL and investigating the central sub-type of SL.

Defining the properties of the transformation from the given labels to learnable targets for an SL task as ‘carelessly designed’ and ‘carefully designed’ two types, we further categorize SL into three narrower sub-types. The three sub-types include precisely supervised learning (PSL), moderately supervised learning (MSL), and precisely and moderately combined supervised

learning (PMCSL). A short illustration for this narrower categorization is presented in Fig. 1. PSL concerns the situation where the given labels are precisely fine. In this situation, we can carelessly design a transformation to obtain the learnable targets from the given labels. In other words, the given labels can be viewed as learnable targets to a large extent. PSL is the most classic sub-type of SL, and typical tasks include simple task like image classification [8] and complicated task like image semantic segmentation [9]. MSL concerns the situation where the given labels are ideal, but due to the simplicity in annotation of the given labels, careful designs are required to transform the given labels into learnable targets for the learning task. This situation is different from the classic PSL, since the given labels must be carefully transformed into learnable targets for the learning task, which would otherwise lead to poor performance. This situation is also different from WSL since the given labels are complete, exact and accurate. Typical MSL tasks include cell detection (CD) [3] and line segment detection (LSD) [4]. PMCSL concerns the situation where the given labels contain both precisely fine and ideal but simple annotations. Usually, PMCSL consists of a few PSL and MSL sub-tasks. Typical PMCSL tasks include visual object detection [10], facial expression recognition [11] and human pose identification [12]. More detailed characteristics of PSL, MSL and PMCSL are provided in Section 3.

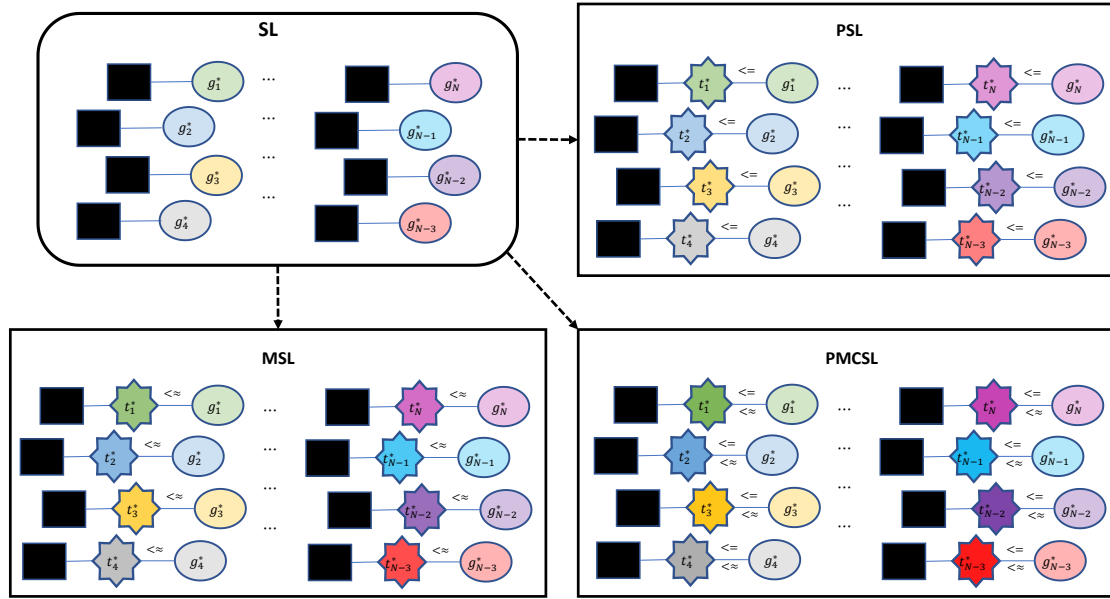


Fig. 1. Narrower categorization for supervised learning (SL). The three sub-types of SL include precisely supervised learning (PSL), moderately supervised learning (MSL), and precisely and moderately combined supervised learning (PMCSL). Black rectangles denote events/entities in the training data set; coloured ellipses indicate the labels assigned to corresponding events/entities; coloured polygons signify learnable targets transformed from corresponding labels. \leq/\approx denote 'carelessly designed' or 'carefully designed' transformation.

In the three narrower sub-types, MSL counts for the majority of SL, due to the fact that PSL only counts for a small proportion of SL and MSL is an essential part of PMCSL which account for the most proportion of SL. As a result, MSL plays the central role in the field of SL. Although solutions have been intermittently proposed for different MSL tasks, currently, insufficient researches have been devoted to clearly defining and systematically analysing MSL, so as to reveal the details concealed by the abstractness of the definition of SL. To fill in this gap, we present

comprehensive elaborations for MSL from the perspectives of definition, framework and generality. In this paper, we formulate MSL to clearly define it and present a generalized framework to systematically analyse MSL. In addition, we also show the generality exist among different MSL solutions; that is, solutions for a wide variety of MSL tasks can be abstractly unified into the presented MSL framework. Details of the definition, framework and generality presented for MSL are provided in Section 4. Eventually, based on the definition, framework and generality presented for MSL, we discuss the key points of constructing fundamental MSL solutions and the key problems of developing better MSL solutions to reveal the details that are critical to building the appropriate solutions but concealed by the abstractness of the definition of SL. Specific discussions can be found in Section 5.

As an application engineer who uses deep learning technology to promote the development of AI applications, in addition to chasing the state-of-the-art result for a problem to be solved, viewing the problem from the mathematicians' vision is as well critical to discover, evaluate and select appropriate solutions for the problem, especially when deep learning has been becoming increasingly standardized and reaching its limits in many AI applications. However, currently, most AI application engineers primarily focus on chasing the state-of-the-art results for a problem to be solved, and few pay attention to viewing the problem from the mathematicians' vision. So, the question is how is the mathematicians' vision? There is a generalized answer to this question, which has been presented by the Chinese mathematician Jingzhong Zhang [13]: "Mathematicians' vision is abstract. Those we think are different, they seem to be the same. Mathematicians' vision is precise. Those we think are the same, they seem to be very different. Mathematicians' vision is clear and sharp. They continue pursuing mathematical conclusions that we feel very satisfied with. Mathematicians' vision is dialectical. We think one is one and two is two, but they often focus on what is unchanging in the changing and what is changing in the unchanging." While presenting the definition, framework and generality of MSL, this paper as well establishes a specific example for understanding of this generalized answer, which can be a tutorial for AI application engineers to refer to viewing a problem to be solved from the mathematicians' vision.

2. Preliminary

Formally, the task of learning with supervision is to learn a function $f: d \mapsto g^*$ from a training data set \mathcal{T} . Usually, d denotes a set of events/entities, g^* represents the given labels corresponding to d , and the training dataset \mathcal{T} consists of the events/entities d with their labels g^* . In the current literature, there are two main types: supervised learning (SL) and weakly supervised learning (WSL). Usually, these two types are distinguished according to the properties (completeness, exactness and accuracy) of the labels prepared for the events/entities in the training data set \mathcal{T} . Some basic notations that appear in this paper are summarized in Table 1.

2.1 Supervised learning

SL learns predictive models with complete, exact and accurate labels. Specifically, the training data set $\mathcal{T} = \{(d_1, g_1^*), \dots, (d_N, g_N^*)\}$, where N is the number of events/entities and each d_n has a label g_n^* that can ideally describe its ground-truth. Based on such prepared training data sets, SL has been widely adopted to solve fundamental tasks such as image classification, visual object tracking, visual object detection, and image semantic segmentation in the field of computer vision [14–17] and other applications [18].

Table 1. Summary of basic notations used in this paper.

Notation	Meaning
f	a function that maps from a to b
\mathcal{T}	a training data set that consists of events/entities with corresponding labels
d	a set of events/entities
g^*	Labels corresponding to events/entities
N	number of events/entities in the training data set \mathcal{T}
t^*	learnable targets, a transformation of g^*
\leq/\approx	non-parameterized/parameterized transformation
\wedge/\vee	and/or
t	predicted targets of events/entities
g	final predicted labels, a re-transformation of t
I	space of learnable targets t^*
J	space of predicted targets t
H	space of final predicted labels g
$\omega^d/\omega^i/\omega^e$	parameters for Decoder/Inferer/Encoder
$M^d/M^i/M^e$	space of parameters for Decoder/Inferer/Encoder
\mathcal{F}	a 2D image lattice
p	a 2D point in image lattice \mathcal{F}
P	a set of cell centres labelled in \mathcal{F}
L	a set of line segments labelled in \mathcal{F}
D	an input image lattice

2.2 Weakly supervised learning

WSL attempts to learn predictive models with incomplete, inexact or inaccurate labels [19]. Learning with incomplete labels focuses on the situation where only a small amount of ideally labelled data is given to train a predictive model, while abundant unlabelled data are available. In this situation, the ideally labelled data are insufficient to learn a good model. Active learning [20] and semi-supervised learning [21] are two typical techniques for this situation. Specifically, the training data set $\mathcal{T} = \{(d_1, g_1^*), \dots, (d_J, g_J^*), d_{J+1}, \dots, d_N\}$, where only a small portion $\{d_j | j \in \{1, \dots, J\}\}$ of d has labels. Learning with inexact labels concerns using only coarsely labelled data that is not as exact as the ideally labelled data to learn a predictor. The typical technique for this situation is multi-instance learning [22]. Specifically, the training data set $\mathcal{T} = \{(d_1, g_1^*), \dots, (d_N, g_N^*)\}$, where $d_n = \{d_{n,1}, \dots, d_{n,M_n}\} \subseteq d$ is called a bag, $d_{n,m} \in d$ ($m \in \{1, \dots, M_n\}$) is an instance, and M_n is the number of instances in d_n . For a two-class classification multi-instance learning task where $t^* = \{y, n\}$, d_n is a positive bag, i.e., $t_n^* = y$, if there exists $d_{n,p}$ that is positive, while what is known is only $p \in \{1, \dots, M_n\}$. The goal is to predict labels for unseen bags. Learning with inaccurate labels focuses on using data the labels of which compared with the ideal labels may contain errors to train a reasonable predictive model. A typical technique for this situation is learning with noisy labels [23]. Specifically, the training data set $\mathcal{T} = \{(d_1, (g_1^* + \Delta_1)), \dots, (d_N, (g_N^* + \Delta_N))\}$, where $(g_n^* + \Delta_n)$ is the given ground-truth label, which consists of an accurate label g_n^* and a label error Δ_n . With the efficiency and lower cost of the data labelling process, WSL has become popular for addressing many complicated SL tasks that requires labour extensive annotations, such as various medical image analysis tasks [24–

3. Narrower Sub-types of Supervised Learning

The categorization in the preliminary section simply takes into consideration the properties (completeness, exactness and accuracy) of the labels prepared for the training data set. However, in practice, we usually cannot directly learn a function $f: d \mapsto g^*$ for an SL task. We must build a transformation from given labels g^* to learnable targets t^* , and learn a function $f: d \mapsto t^*$. In this section, by taking the properties of the transformation from g^* to t^* into consideration, we expand the categorization for SL. Usually, a transformation for an SL task is coupled with a label re-transformation from the predicted targets of the learnt function f to the final predicted labels. Since a label re-transformation commonly consists of the reverse operations corresponding to its coupled transformation, in this section, we assume that the properties of the label re-transformation remain the same as the properties of its coupled target transformer and give no additional discussions.

3.1 Properties of transformation

We classify the transformations of solutions for SL tasks into ‘carelessly designed’ and ‘carefully designed’ two types. Intrinsically, we define that a transformation is the ‘carelessly designed’ type if it is non-parameterized while a transformation is ‘carefully designed’ type if it is parameterized, due to the fact that a non-parameterized transformation simply requires careless designs while a parameterized transformer must require careful designs. That a non-parameterized transformation simply requires careless designs is because it can generate a type of the learnable targets that can be considered to be optimal. However, that a parameterized transformation must require careful designs is because adjusting its parameters can generate various types of learnable targets from which the optimal type of learnable targets need to be found. To formally summarize the properties of a transformation, we present Definition 1 as follow.

Definition 1. For the given labels g^* , the learnable targets generated by a ‘carelessly designed’ transformation are

$$t^* = \{t_n^* | t_n^* \leq g_n^*, n \in \{1, \dots, N\}\},$$

where \leq signifies the non-parameterized transformation of t_n^* from g_n^* and the type of targets t^* can be considered as optimal; and the learnable targets generated by a ‘carefully designed’ transformation are

$$t^* = \{t_n^* | t_n^* \approx g_n^*, n \in \{1, \dots, N\}\},$$

where \approx signifies the parameterized transformation of t_n^* from g_n^* and the optimal type of targets t^* need to be found by adjusting the parameters.

3.2 Sub-types of SL

Taking into consideration the two properties of a transformation presented in Definition 1, we further classify SL into three narrower sub-types: precisely supervised learning (PSL), moderately supervised learning (MSL), and precisely and moderately combined supervised learning (PMCSL).

3.2.1 Precisely supervised learning

PSL concerns the situation where the given labels g^* in the training data set have precisely fine labels. In this situation, we can simply construct a non-parameterized transformation with

careless designs to obtain the learnable targets t^* from g^* . Image classification [8] and image semantic segmentation [9] are two typical PSL problems.

In a C -class image classification task, the given ground-truth label for the class of an image can usually be transformed into a learnable target using a C -bit vector. In this vector, the bit corresponding to the given ground-truth label is set to 1, and the remaining bits are set to 0. Similarly, for a C -class image semantic segmentation task, each pixel point in the given ground-truth label for the semantic objects in an image can be transformed into a value at the same pixel point in the learnable target. The transformed value can be a one-hot vector in classification or real-value response in regression, corresponding to its predefined class in the given ground-truth label. We can note that the transformations for these two PSL tasks are non-parameterized and can be simply built with careless designs. In other words, to some extent, the given labels g^* can be viewed as learnable targets due to their precise fineness.

3.2.2 Moderately supervised learning

MSL focuses on the situation where the given labels g^* in the training dataset are ideal while possessing to some extent extreme simplicity. This situation is different from PSL since the simplicity of g^* makes directly learning from the learnable targets of its carelessly designed transformation probably impossible or leads to very poor performance. MSL is also different from WSL, as the given labels are not incomplete, inexact or inaccurate but ideal. Since the given labels are not strong enough for PSL but also not weak enough for WSL, we refer to this situation as MSL. Due to the simplicity of g^* , in this situation, the transformation from g^* to learnable targets t^* usually is parameterized and must require careful designs. Cell detection (CD) [3] and line segment detection (LSD) [4] with point labels are two typical MSL tasks.

In the CD task, the given labels for cells in an image lattice are simply a set of 2D points indicating the cell centres. In the LSD task, the given labels for line segments in an image lattice are simply a set of tuples, each of which contains two 2D points. The connection between the two 2D points of a tuple indicates a line segment in an image lattice. As the given labels for these two tasks are extremely simple, directly transforming them into learnable targets, in which pixel points corresponding to g^* are set as foreground objects and the rest are set as background objects, will make the learning task impossible or lead to very poor performance. A more appropriate transformation which are restricted by a number of parameters (a parameterized transformation) can be used to alleviate this situation. However, adjusting the parameters of this parameterized transformation can result in various learnable targets that can significantly affect the performance of the final solution for an MSL task. As a result, it is usually difficult to find the optimal learnable targets from the parameterized transformation for an MSL task. Thus, an appropriately parameterized transformation for an MSL task must require careful designs to be constructed.

3.2.3 Precisely and moderately combined supervised learning

PMCSL concerns the situation where the given labels g^* contain both precise and moderate annotations. In this situation, the transformation is usually built to have a mixture of properties of both the transformations designed for PSL and MSL tasks. Typical PMCSL tasks include visual object detection [10], facial expression recognition [11] and human pose identification [12]. Each of these tasks usually consists of a few PSL and MSL problems.

In the visual object detection task, the given labels for the objects in an image lattice are usually a set of tuples, each containing a class name and a bounding box to indicate the category of an object and its position. Currently, deep convolutional neural network-based [8, 27–31] one-

stage approaches (YOLO [32–35], SSD [36] and RetinaNet [6]) and two-stage approaches (RCNN [37], SPPNet [38], Fast RCNN [39], Faster RCNN [40] and FPN [5]) are the state-of-the art solutions for this task. The transformations of these solutions usually have a parameterized sub-transformation and a non-parameterized sub-transformation. The parameterized sub-transformation is responsible for pre-defining a set of reference boxes (a.k.a. anchor boxes) with different sizes and aspect ratios at different locations of an image lattice. The sizes and aspect ratios can be adjusted to generate various reference boxes. These reference boxes are used to indicate the probabilities of corresponding areas as objects in an image lattice. The non-parameterized sub-transformation is responsible for transforming the reference boxes obtained from the parameterized sub-transformation into their categories and locations according to the ground-truth class names and ground-truth bounding boxes labelled in an image lattice. In facial expression recognition [11] and human pose identification [12] tasks, the detection of landmarks of a face or a human is the primary problem. The given labels for the landmarks of a face or a human in an image are usually a set of tuples, each of which contains a 2D vector and a number to indicate the position and category of the landmark. The transformation of possible solution for the detection of landmarks also has a parameterized sub-transformation and a non-parameterized sub-transformation. Basically, the detection of landmarks consists of two sub-problems: locating the landmarks and classifying the located landmarks. The parameterized sub-transformation, which is similar to the target transformers of solutions for pure MSL problems, aims to generate targets for locating landmarks, and the non-parameterized sub-transformation is responsible for producing targets for classifying the located landmarks. These typical problems show that the transformation for PMCSL enjoys a mixture of properties of the transformations for pure PSL and pure MSL.

Training Data Set		Target Transformation	
SL	$\mathcal{T} = \{(d_1, g_1^*), \dots, (d_N, g_N^*)\}$	$t^* = \{t_n^* t_n^* \leq g_n^*, n \in \{1, \dots, N\}\}$	PSL
		$t^* = \{t_n^* t_n^* \approx g_n^*, n \in \{1, \dots, N\}\}$	MSL
		$t^* = \{t_n^* t_n^* \leq \wedge \approx g_n^*, n \in \{1, \dots, N\}\}$	PMCSL
Incomplete	$\mathcal{T} = \{(d_1, g_1^*), \dots, (d_j, g_j^*), d_{j+1}, \dots, d_N\}$	$t^* = \{t_n^* t_n^* \leq \vee \approx g_n^*, n \in \{1, \dots, N\}\}$	WSL
Inexact	$\mathcal{T} = \{(d_1, g_1^*), \dots, (d_N, g_N^*)\},$ $d_n = \{d_{n,1}, \dots, d_{n,M_n}\} \subseteq d,$ $d_{n,m} \in d \ (m \in \{1, \dots, M_n\})$		
Inaccurate	$\mathcal{T} = \{(d_1, (g_1^* + \Delta_1)), \dots, (d_N, (g_N^* + \Delta_N))\}$		

Fig. 2. Deeper categorization for SL. \leq/\approx denote non-parameterized ('carelessly designed') / parameterized ('carefully designed') transformation. \wedge/\vee denote and/or.

3.3 Analysis

In fact, the three sub-types (PSL, MSL and PMCSL) of SL can be converted between each other by changing the modeling methods of the transformations for their solutions. However, once the transformation for a possible solution has been constructed, the sub-type of the corresponding SL

task is clearly clarified. In other words, the constructed transformation of a possible solution for an SL task fundamentally determines the sub-type of this SL task, which is crucial to building the appropriate solution for the task. Additionally, taking Definition 1 into consideration, WSL can also be classified into narrower sub-types. However, here we only focus more on the sub-types of SL, since SL is more fundamental than WSL in the field of learning with supervision and the sub-types of SL can naturally adjust to WSL. As a result, a deeper categorization for SL is presented as Fig. 2.

4. Moderately Supervised Learning

In this section, we comprehensively illustrate MSL from the perspectives of the definition, framework and generality to reveal the details that can be critical to building the appropriate solutions but concealed by the abstractness of the definition of SL.

4.1 Definition

Let us consider the situation where the given labels of a number of training events/entities are ideal (complete, exact and accurate) but possess simplicity. Specifically, with the given simple labels g^* , the ultimate goal of the learning task here is to find the final predicted labels g that minimize the error against g^* . Regarding this situation as a classic SL problem, we can define the objective function as

$$\min_g \ell(g, g^*), \quad (0-1)$$

where $\ell(\cdot, \cdot)$ refers to a loss function that estimates the error between two given elements. The smaller the value of this function is, the better the found g is.

Due to the simplicity of g^* , we must carefully build a transformation that transforms g^* into learnable targets t^* . On the basis of the transformed learnable targets t^* , we build a learning function that maps events/entities t^* to the predicted targets and find those predicted targets t that minimize the error against t^* . Based on the found predicted targets t , we then carefully build a label re-transformation that re-transforms t into the final predicted labels and find those predicted labels g that can minimize the error against the labels g^* . We assume t^* can be constructed by ‘decoding’ g^* as the learnable targets t^* are more informative than the labels g^* , the predicted targets t can be obtained by ‘inferring’ d , and g can be constructed by ‘encoding’ t as the final predicted labels g are less informative than the predicted targets t . Formally, we specify the following definition for MSL:

$$\begin{aligned} t^* &= \text{decoder}(g^*) \quad t^* \in I, \\ t &= \text{inferrer}(d) \quad t \in J, \quad \min_{t \in J} \ell^i(t, t^*), \\ g &= \text{encoder}(t) \quad g \in H, \quad \min_{g \in H} \ell^e(g, g^*), \end{aligned} \quad (0-2)$$

where *decoder* denotes the transformation, *inferrer* denotes the learning function f , *encoder* denotes the label re-transformation, and I , J and H denote the spaces of learnable targets t^* , predicted targets t and final predicted targets g .

4.1.3 Analysis

Comparing Eq. (0-2) with Eq. (0-1), we can note that, by taking into consideration the properties of the transformation from the given labels to learnable targets, the definition specified for MSL proves that some details are indeed concealed by the abstractness of the definition of SL.

4.2 Framework

On the basis of the specified definitions for MSL, in this section, we present a generalized MSL framework. The outline of the presented MSL framework is shown as Fig. 3, in which basic components for constructing a fundamental MSL solution and basic procedures of mutual collaborations among the basic components are depicted.

4.2.1 Basic component

The decoder transforms the given simple labels g^* into learnable targets t^* . Commonly, the decoder is built on the basis of prior knowledge which is parameterized by ω^d . Abstractly, we obtain the learnable targets t^* by

$$t^* = \text{decoder}(g^*; \omega^d). \quad (1)$$

The inferrer models the map between the events/entities d and corresponding learnable targets t^* . Usually, the inferrer is built on the basis of machine learning techniques and is parameterized by ω^i . Abstractly, we obtain the predicted targets t by

$$t = \text{inferred}(d; \omega^i). \quad (2)$$

The encoder re-transforms the predicted targets t of the inferrer into the final predicted labels g . Coupled with the decoder, the encoder is built on the basis of the decoder's output t^* which is parameterized by ω^e . Abstractly, we obtain the final predicted labels g by

$$g = \text{encoder}(t; \omega^e). \quad (3)$$

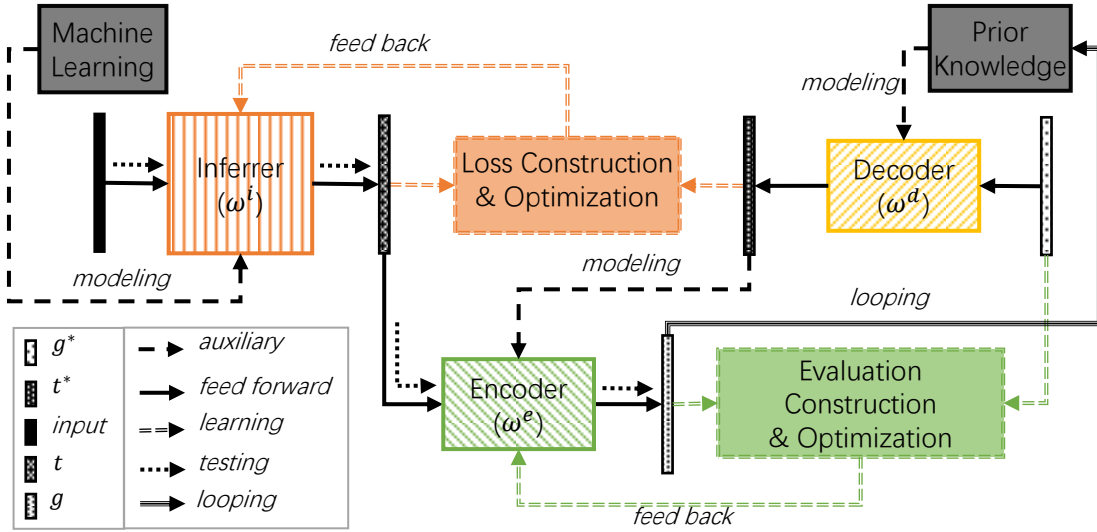


Fig. 3. Generalized MSL framework. Basic components: decoder, inferrer and encoder.

4.2.2 Basic procedure

Learning The learning procedure aims to optimize the parameters ω^i and ω^e for the inferrer and encoder, respectively, under the prerequisite of a decoder that is empirically initialized with $\overline{\omega^d}$. Specifically, we express the learning procedure as

$$\bar{t}^* = \text{decoder}(g^*; \overline{\omega^d}), \quad (4-1)$$

$$\widetilde{\omega^i} = \arg \min_{\omega^i \in M^i} \frac{1}{N} \sum_{n=1}^N \ell^i(\text{inferred}(d_n; \omega^i), \bar{t}_n^*), \quad (4-2)$$

$$\widetilde{\omega^e} = \arg \min_{\omega^e \in M^e} \frac{1}{N} \sum_{n=1}^N \ell^e(\text{encoder}(t_n; \omega^e), g_n^*), \quad (4-3)$$

where M^i and M^e specify the parameter spaces of ω^i and ω^e , respectively, and N is the number of training events/entities.

Looping As the optimization of the parameters (ω^i , ω^e) of both the inferrer and encoder is conducted under the prerequisite of the decoder parameterized by ω^d , a change in the decoder can significantly affect the optimization of ω^i and ω^e , which will eventually be reflected in the final predicted labels g . In fact, prior knowledge can be enriched by analysing the predicted labels g of the current solution. The enriched prior knowledge can help us to model and initialize a better decoder. Thus, in practice, we commonly loop several times to adjust the decoder and restart the training for a possibly better solution. Specifically, we express the looping procedure as

$$\widetilde{\omega}^d = \arg \min_{\omega^d \in M^d} l(g|\omega^d, g^*), \quad (5)$$

where M^d signifies the parameter space of ω^d and $g|\omega^d$ denotes that the final predicted labels g are obtained by optimizing the parameters (ω^i , ω^e) of both the inferrer and encoder under the prerequisite of the decoder initialized with ω^d .

Testing As shown in Fig. 2, testing starts from input d , passes through the inferrer and encoder, and ends at g . Specifically, the testing procedure can be expressed as

$$t = \text{inferrer}(d; \widetilde{\omega}^i | \widetilde{\omega}^d), \quad (6-1)$$

$$g = \text{encoder}(t; \widetilde{\omega}^e | \widetilde{\omega}^d), \quad (6-2)$$

where $\widetilde{\omega}^i | \widetilde{\omega}^d$ and $\widetilde{\omega}^e | \widetilde{\omega}^d$ are the parameters of the inferrer and encoder optimized under the prerequisite of the decoder initialized with $\widetilde{\omega}^d$ found by the looping procedure.

4.2.3 Analysis

From Eq. (1) to (6), we can note that the generalized framework presented for MSL in fact reveals the key points of constructing fundamental MSL solutions and the key problems of developing better MSL solutions, which are concealed by the roughness of SL category. The key points of constructing fundamental MSL solutions can be summarized as modelling the three basic components (decoder, inferrer and encoder), and the key problems of developing better MSL solutions can be summarized as the learning and looping procedures to optimize the three basic components. The decoder is responsible for transforming the given labels into learnable targets. Usually, it is built and optimized on the basis of prior knowledge. The inferrer is responsible for mapping events/entities to corresponding learnable targets. Usually, it is built and optimized on the basis of machine learning techniques. The encoder is responsible for transforming the predicted targets of the inferrer into final predicted labels. Usually, the encoder is built and optimized on the basis of the decoder.

4.3 Generality

Although solutions have been intermittently proposed for different MSL tasks, little work has explored the generality of different MSL tasks, due to the lack of a clear problem definition and systematic problem analysis. In this subsection, based on the specified definition and presented framework for MSL, we show that generality exists among cell detection (CD) [3] and line segment detection (LSD) [4], which are two typical MSL tasks according to the definition of MSL and have large differences in application scenarios. Following the presented framework for MSL, we review and rebuild the solutions proposed in [3, 4] for these two largely different typical MSL problems to show that generality exist in their solutions.

4.3.1 Cell detection

Let \mathcal{F} be a 2D image lattice (e.g., 800×800). The moderate supervision information for the

CD task uses a point $p_j = (x_j, y_j)$ with offsets x_j and y_j , respectively, to represent the cell centre in \mathcal{F} . In this situation, the ground-truth label in \mathcal{F} is denoted by $P = \{p_j | j = \{1, \dots, m\}\}$. Some example images and corresponding labels are given in Fig. 4.

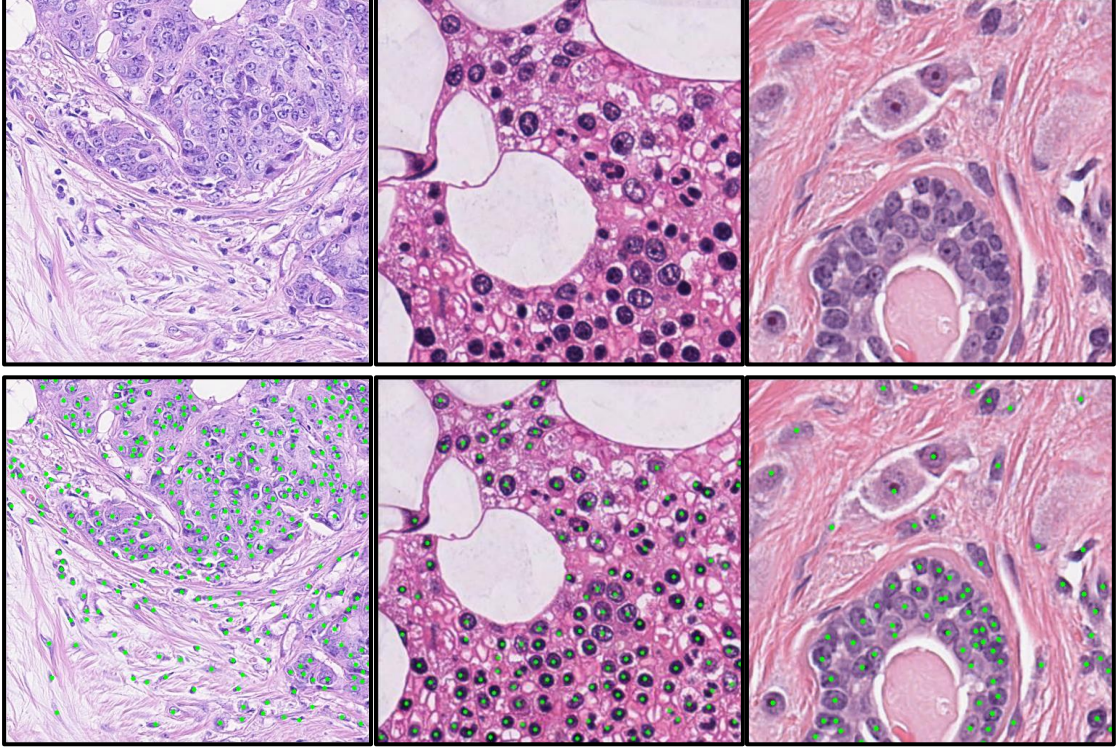


Fig. 4. Example images and corresponding labels for cell detection [3, 41, 42]. Top row: original images. Bottom row: labels shown on original images.

(1) Decoder

The decoder transforms P labelled in an image lattice \mathcal{F} into a structured learnable target. It first assigns each pixel point $p \in \mathcal{F}$ to the nearest cell centre point in P to partitions \mathcal{F} into m regions. Each region serves as a supportive area for a cell centre point. Then, by projecting its supportive region into a 1D real-valued representation, it transforms each cell centre p_j in P into a structured representation.

Modelling For assignment of a pixel point $p \in \mathcal{F}$ to its nearest cell centre point, we use Euclidian distance to define the distance between p and a candidate cell centre point p_j as

$$dis(p, p_j) = \sqrt{(p - p_j)^2} = \sqrt{(x - x_j)^2 + (y - y_j)^2}.$$

The supportive region for cell centre point p_j is denoted by

$$R(p_j) = \{p | p \in \mathcal{F}; dis(p, p_j) < dis(p, p_k), \forall k \neq j, p_k \in P\}.$$

Then, we define the transformation of each pixel point p in a supportive region $R(p_j)$ into a real-valued representation by

$$a_j(p) = e^{\left(1 - \frac{dis(p, p_j)}{dis_j}\right)} - 1, \quad p \in R(p_j), \quad dis_j = \max dis(p, p_j).$$

Using a_j , we can transform a cell centre p_j into a structured 1D representation. This transformation function is applied over the entire P labelled in image lattice \mathcal{F} as

$$a: P \xrightarrow{\text{transforming}} \mathbb{R},$$

$$p_j \rightarrow a_j(R(p_j)), \quad p_j \in P.$$

For simplicity, the structured target generated by the transformation function a can be denoted by

$$E = \{a_j(R(p_j)) \mid p_j \in P; j = \{1, \dots, m\}\}.$$

Parameterization Using the transformation function a , we can transform P labelled in \mathcal{F} into a structured target without setting any specific parameters. However, the structured target transformed by this parameter-free model is redundant since many pixel points far from a line segment can also be assigned as being among its supportive points, which we believe is unnecessary. Note that φ is the parameter for adjusting the selection of necessary pixel points in \mathcal{F} . We parameterize and rewrite the supportive region for cell centre point p_j as

$$R(p_j; \varphi) = \begin{cases} R_+(p_j; \varphi) = \{p \mid p \in R(p_j); \text{dis}(p, p_j) < \varphi; \} \\ R_-(p_j; \varphi) = \{p \mid p \in R(p_j); \text{dis}(p, p_j) \geq \varphi; \} \end{cases}$$

Then, the function for transforming each pixel point p in $R(p_j; \varphi)$ into a real-valued representation is rewritten as

$$a_j(p; \{\varphi, \alpha\}) = \begin{cases} e^{\alpha(1 - \frac{\text{dis}(p, p_j)}{\varphi})} - 1 & \text{if } p \in R_+(p_j; \varphi), \\ 0 & \text{if } p \in R_-(p_j; \varphi) \end{cases}$$

where α is a parameter added to control the exponential decrease rate of φ close to the centre point.

Generalization Decoding model: $\{R, a\}$; Input: $g^* = P$; Parameter: $\omega^d = \{\varphi, \alpha\}$; Output: $t^* = E$. Referring to Eq. (1), the transforming process of the decoder for the CD task can be defined as

$$E = \underset{\{R, a\}}{\text{decoder}}(P; \{\varphi, \alpha\}). \quad (\text{CD-1})$$

Fig. 5 illustrates how the decoder transforms the ground-truth label into a learnable target for the CD task.

(2) Inferer

Modelling A deep convolutional neural network (DCNN) is employed to model the inferer for mapping an input image lattice D to an indirect target G . Define $\{f_o\}_{o=1}^O$ as the transformation for each of the O layers from the DCNN architecture. The mapping function of the inferer can be denoted by

$$\psi = f_o \circ f_{o-1} \circ \dots \circ f_1.$$

Given one input image lattice D , the network computes the output G as

$$G = \psi(D).$$

Parameterization We assume $\{f_o\}_{o=1}^O$ are parameterized by $\{\theta_o\}_{o=1}^O$. The corresponding θ_o has distinct forms for different types of f_o . The output computation of the network is rewritten by

$$G = \psi(D; \theta),$$

$$\theta = \{\theta_1, \dots, \theta_O\}.$$

Generalization Inferring model: $\{\psi\}$; Input: $d = D$; Parameter: $\omega^i = \{\theta\}$; Output: $t = G$. Referring to Eq. (2), the Inferer for the CD task can be abbreviated as

$$G = \underset{\{\psi\}}{\text{inferer}}(D; \{\theta\}). \quad (\text{CD-2})$$

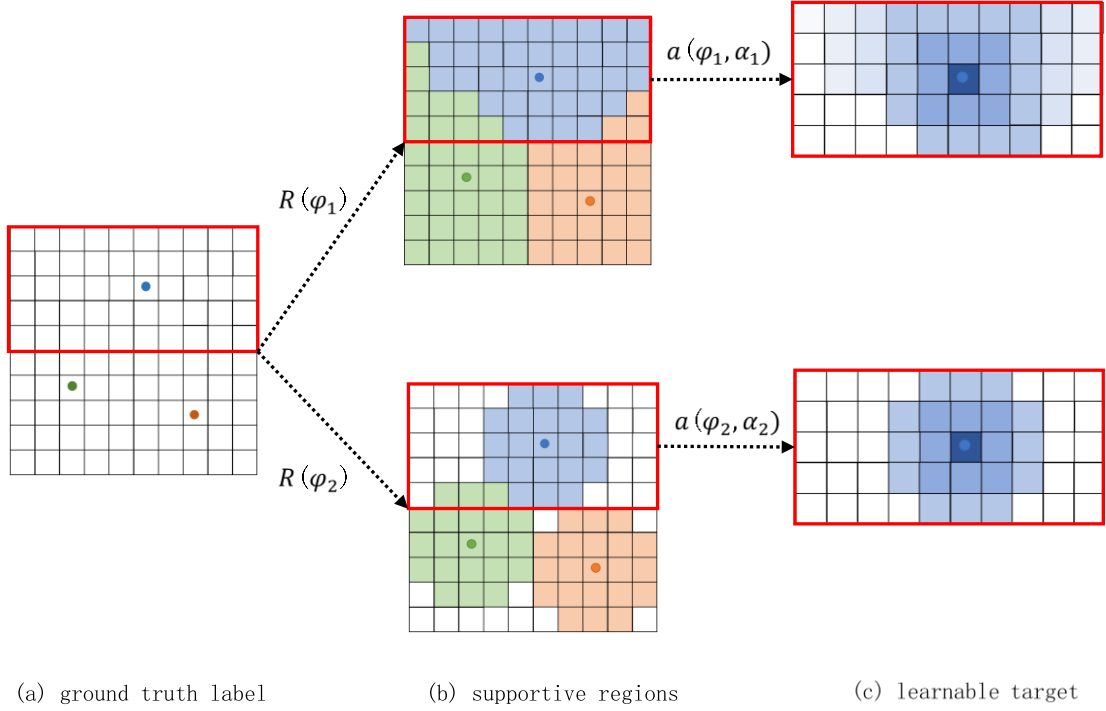


Fig. 5. Illustration of the transforming process of the decoder for the CD task. (a) The given ground-truth label is a 10×10 image lattice in which the centres of three cells are labelled. (b) Supportive regions generated during the transforming process of the decoder. (c) Learnable target generated by transforming supportive regions into a structured representation. The top rows and bottom rows of (a) and (c) are two transformations of the decoder by adjusting its parameters.

(3) Encoder

Modelling Since the decoder is built to respond maximally at the cell centres, the inferer is built to minimize the error between its output G and the output E of the decoder. Thus, by finding local maxima points in the lattice G , we can theoretically re-transform the structured prediction into the detected cell centres. For each point $p = (x, y)$ in lattice G , we define p as a local maxima point if the values at its neighbours $N = \{(x, y - 1), (x, y + 1), (x - 1, y), (x + 1, y)\}$ are smaller than or equal to the value at point p , which can be expressed as

$$\phi(p) = \begin{cases} p & \text{if } G(p) \geq G(p_n), \forall p_n \in N \\ (-1, -1) & \text{otherwise} \end{cases}$$

This re-transformation function is applied over the whole lattice G

$$\phi: G \xrightarrow{\text{re-transforming}} \mathbb{R}^2, \\ p \rightarrow \phi(p), \quad p \in G.$$

As a result, the cell centres detected by the re-transformation function ϕ can be denoted as

$$C = \{p | p \in G; \phi(p) \neq (-1, -1)\}.$$

Parameterization Since noise information appears in the raw output of the inferer, we apply a small threshold $\varepsilon \in [0, 1]$ to remove values smaller than $\varepsilon \cdot \max(G)$. We parameterize and

rewrite the re-transformation function as

$$\phi(p, \varepsilon) = \begin{cases} \text{true} & \text{if } G(p) \geq \varepsilon \cdot \max(G) \cap G(p) \geq G(p_n), \forall p_n \in N \\ \text{false} & \text{otherwise} \end{cases}$$

Optimizing ε can balance between the recall and precision of the final cell detection.

Generalization Encoder model: $\{\phi\}$; Input: $t = G$; Parameter: $\omega^e = \{\varepsilon\}$; Output: $g = C$. Referring to Eq. (3), the encoder for the CD task can be abbreviated as

$$C = \text{encoder}_{\{\phi\}}(G; \{\varepsilon\}). \quad (\text{CD-3})$$

(4) Learning

Referring to Eq. (4), in the learning procedure for the CD task, we first empirically initialize the decoder with $\{\bar{\varphi}, \bar{\alpha}\}$ and utilize the initialized decoder to transform P labelled in an image lattice \mathcal{F} into a structured target by

$$\bar{E} = \text{decoder}_{\{R, a\}}(P; \{\bar{\varphi}, \bar{\alpha}\}). \quad (\text{CD-4-1})$$

Then, we optimize the parameters of the inferrer by

$$\begin{aligned} \tilde{\theta} &= \arg \min_{\theta \in M^i} \frac{1}{N} \sum_{n=1}^N \ell^i \left(\text{inferred}_{\{\psi\}}(D_n; \{\theta\}), \bar{E} \right), \\ \ell^i \left(\text{inferred}_{\{\psi\}}(D; \{\theta\}), \bar{E} \right) &= \frac{1}{2} \sum_{p \in \mathcal{F}} (\beta G(p) + \gamma \bar{G})(G(p) - \bar{E}(p)), \end{aligned} \quad (\text{CD-4-2})$$

where β and γ are predefined constants used to tune the losses. The parameters of the encoder are optimized by

$$\begin{aligned} \tilde{\varepsilon} &= \arg \min_{\varepsilon \in M^e} \frac{1}{N} \sum_{n=1}^N \ell^e \left(\text{encoder}_{\{\phi\}}(C_n; \{\varepsilon\}), P_n \right), \\ \ell^e \left(\text{encoder}_{\{\phi\}}(C; \{\varepsilon\}), P \right) &= \frac{(C \cup P) - (C \cap P)}{C \cup P}. \end{aligned} \quad (\text{CD-4-3})$$

(5) Looping

Usually, we loop several times to find relatively optimal parameters for the decoder. Referring to Eq. (5), the looping procedure for the CD task can be specified as

$$\begin{aligned} \{\tilde{\varphi}, \tilde{\alpha}\} &= \arg \min_{\{\varphi, \alpha\} \in M^d} l(C|\{\varphi, \alpha\}, P), \\ l(C|\{\varphi, \alpha\}, P) &= \frac{((C|\{\varphi, \alpha\}) \cup P) - ((C|\{\varphi, \alpha\}) \cap P)}{(C|\{\varphi, \alpha\}) \cup P}, \\ C|\{\varphi, \alpha\} &= \text{encoder}_{\{\phi\}} \left(\text{inferred}_{\{\psi\}}(D; \{\tilde{\theta}\}); \{\tilde{\varepsilon}\} \right). \end{aligned} \quad (\text{CD-5})$$

(6) Testing

Referring to Eq. (6), the testing procedure for the CD task can be specified as

$$G = \text{inferred}_{\{\psi\}}(D; \{\tilde{\theta}\}|\{\tilde{\varphi}, \tilde{\alpha}\}), \quad (\text{CD-6-1})$$

$$C = \text{encoder}_{\{\phi\}}(G; \{\tilde{\varepsilon}\}|\{\tilde{\varphi}, \tilde{\alpha}\}). \quad (\text{CD-6-2})$$

4.3.2 Line segment detection

Let \mathcal{F} be a 2D image lattice (e.g., 800×800). The moderate supervision information for the LSD task uses $l_k = (p_k^s, p_k^e)$ with the two points $p_k^s = (x_k^s, y_k^s)$ and $p_k^e = (x_k^e, y_k^e)$ representing the position of a line segment in \mathcal{F} . In this situation, the ground-truth label for \mathcal{F} is denoted by

$L = \{l_k | k = \{1, \dots, m\}\}$. Some example images and corresponding labels are given in Fig. 6.

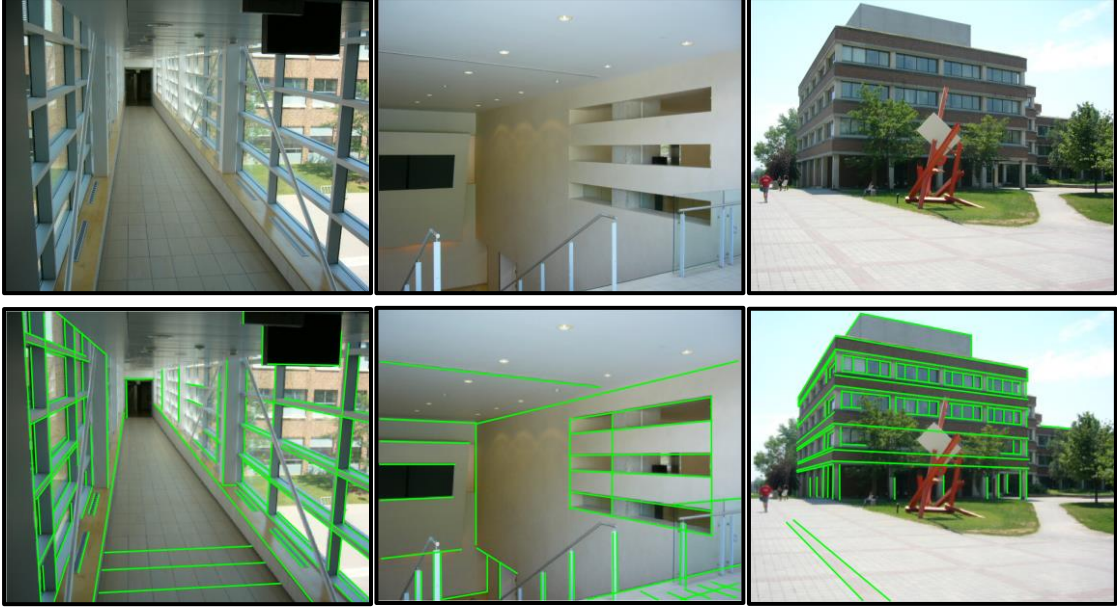


Fig. 6. Example images and corresponding labels for line segment detection [43, 44]. Top row: original images. Bottom row: labels shown on original images.

(1) Decoder

The decoder transforms line segments L labelled in an image lattice \mathcal{F} into a structured learnable target. It first assigns each pixel point $p \in \mathcal{F}$ to the nearest line segment in L , which partitions \mathcal{F} into m regions. Each region serves as a supportive area for a line segment. Then, by projecting its supportive region into a 2D real-valued representation, each line segment l_j in L is transformed into a structured representation.

Modelling For the assignment of a pixel point $p \in \mathcal{F}$ to its nearest line segment, we use a distance function that defines the shortest distance between p and a candidate line segment l_k as

$$dis(p, l_k) = \min_{z \in [0,1]} dis(p, l_k; z) = \min_{z \in [0,1]} \|p_k^s + z \cdot (p_k^e - p_k^s) - p\|_2^2.$$

The value of t associated with the shortest distance between p and l_k is defined as

$$z_p^\sim = \arg \min_{z \in [0,1]} dis(p, l_k; z).$$

The projection point p' of p on l_k is defined as

$$p' = p_k^s + z_p^\sim \cdot (p_k^e - p_k^s).$$

The supportive region for line segment l_k is defined as

$$R(l_k) = \{p | p \in \mathcal{F}; dis(p, l_k) < dis(p, l_j), \forall j \neq k, l_j \in L\}.$$

Then, the transformation of each pixel point p in a supportive region $R(l_k)$ into a structured 2D representation is defined by

$$a_k(p) = p' - p, \quad p \in R(l_k)$$

where the 2D representation vector is perpendicular to the line segment l_k when $t_p^\sim \in (0,1)$.

This transformation function is applied over the whole L labelled in image lattice \mathcal{F} as

$$a: L \xrightarrow{\text{transforming}} \mathbb{R}^2,$$

$$l_k \rightarrow a_k(R(l_k)), \quad l_k \in L.$$

For simplicity, the structured target generated by the transformation function a can be denoted by

$$E = \{a_k(R(l_k)) | l_k \in L; k = \{1, \dots, m\}\}.$$

Parameterization Using the transformation function a , we can transform L labelled in \mathcal{F} into a structured target without setting any specific parameters. However, the structured target transformed by this parameter-free model is redundant since many pixel points far from a line segment can also be assigned as its supportive points, which we believe is unnecessary. Note that φ is the parameter for adjusting the selection of necessary pixel points in \mathcal{F} . We parameterize and rewrite the supportive region for line segment l_k as

$$R(l_k; \varphi) = \begin{cases} R_+(l_k; \varphi) = \{p | p \in R(l_k); d(p, l_k) < \varphi\} \\ R_-(l_k; \varphi) = \{p | p \in R(l_k); d(p, l_k) \geq \varphi\} \end{cases}.$$

Then, the transformation of each pixel point p in a supportive region $R(l_k; \varphi)$ into a structured 2D representation is defined as

$$a_k(p) = \begin{cases} p' - p & p \in R_+(l_k; \varphi) \\ (-x - 1, -y - 1), & p \in R_-(l_k; \varphi) \end{cases}.$$

Generalization decoder model: $\{R, a\}$; Input: $g^* = L$; Parameter: $\omega^d = \varphi$; Output: $t^* = A$. Referring to Eq. (1), we abbreviate the transforming process of the decoder for the LSD task as

$$E = \underset{\{R, a\}}{decoder}(L; \varphi).$$

(LSD-1)

Fig. 7 illustrates how the decoder transforms the ground-truth label into a learnable target for the LSD task.

(2) Inferer

A DCNN is employed to model the inferer for mapping an input image lattice D to an indirect target G , which can be denoted as

$$G = \underset{\{\psi\}}{inferer}(D; \{\theta\}), \quad (\text{LSD-2})$$

where ψ is the mapping function of the inferer and θ are the parameters of ψ .

(3) Encoder

Modelling For each pixel point p in G , we can compute its predicted projection point on a possible line segment by

$$v(p) = p + G(p),$$

where $G(p)$ denotes the predicted 2D vector at pixel point p of G . Its discretized point in the lattice is denoted by

$$v_{\wedge}(p) = \lfloor v(p) + 0.5 \rfloor,$$

where $\lfloor \cdot \rfloor$ represents the floor operation. In addition, if the projected point $v(p)$ is inside a line segment, $G(p)$ provides the normal direction of the line segment going through the point $v(p)$

$$\tau(p) = \arctan2(G_x(p), G_y(p)).$$

Using $v_{\wedge}(p)$, we can rearrange G into a sparse map that records the locations of possible line segments. Such a sparse map is termed a line proposal map, in which a pixel point q collects supportive pixels whose discretized projection points are q . The candidate set of supportive pixels collected by pixel q in the line proposal map is defined by

$$S(q) = \{G(p) | p \in G, v_\wedge(p) = q\}.$$

Thus, using $C(q)$, a line proposal map is defined by

$$Q = \{q | S(q) \neq \emptyset, \forall q \in \mathcal{F}\}.$$

where each pixel point q of Q corresponds to a point on a possible line segment and is associated with a set of supportive pixels $C(q)$ in G . The line proposal map projects the supportive pixels for a line segment into pixels near the line segment.

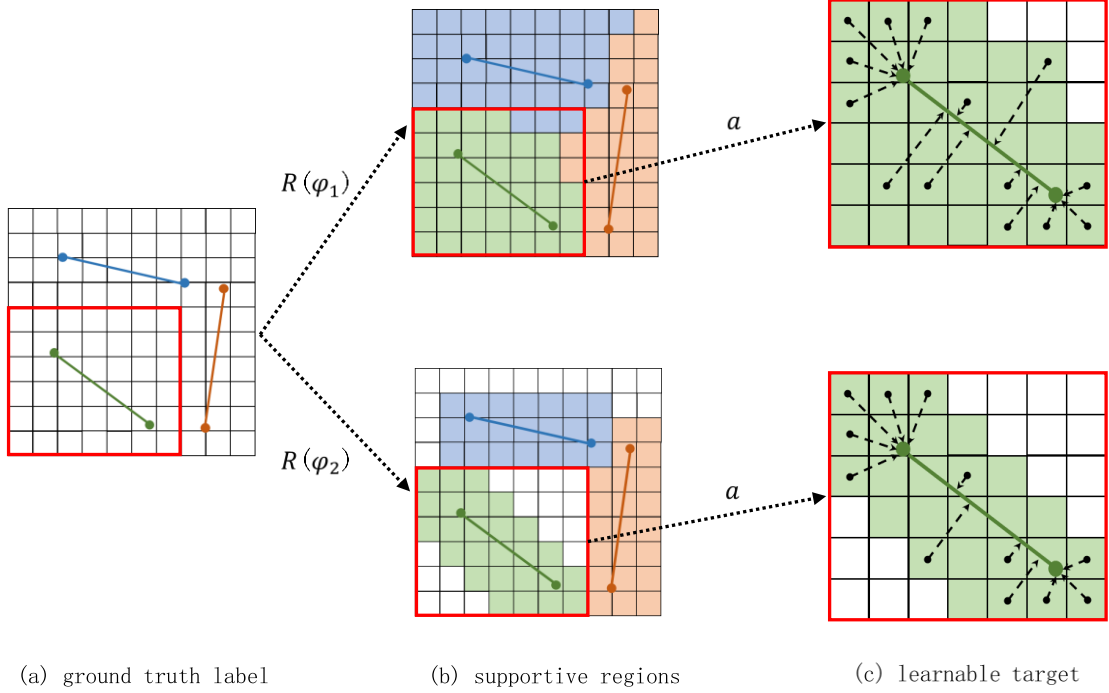


Fig. 7. Illustration of the transforming process of the decoder for the LSD task. (a) The given ground-truth label is a 10×10 image lattice in which the ends of three line-segments are labelled. (b) Supportive regions generated during the transformation process of the decoder. (c) Learnable target generated by transforming supportive regions into a structured representation. The top rows and bottom rows of (a) and (c) are two transformations of the decoder obtained by adjusting its parameters.

With the line proposal map Q , the problem is to group the points of Q into line segments to eventually re-transform the structured prediction into detected line segments. In the spirit of the region growing algorithm used in [45], an iterative and greedy grouping strategy is employed to fit line segments. The procedures of this strategy are as follows.

First, from the line proposal map Q , we obtain the current set of active pixels, each of which has a non-empty candidate set of supportive pixels. We also randomly select a pixel from the set of active pixels and obtain its supportive pixels. This procedure can be denoted by

$$q_0 = \text{random_selection}(Q),$$

$$c_0 = C(q_0).$$

Second, with Q , q_0 , and c_0 , we initialize the points of the current line segment and its supportive pixels and deactivate the points of the current line from Q , which can be denoted by

$$q_c = \{q_0\},$$

$$c_c = \{c_0\},$$

$$Q = deactivate(Q, q_0).$$

Iteratively, from Q , we find more active pixels that are aligned with the current line segment and group these active pixels aligned with points of the current line segment, which can be denoted by

$$s = center_align(Q, q_c, c_c),$$

$$group(q_c, c_c, s) => \begin{cases} end & s = \emptyset \\ \begin{cases} q_c = q_c \cup s \\ c_c = c_c \cup C(s) \\ Q = deactivate(Q_a, s) \end{cases} & otherwise' \end{cases}$$

Finally, we fit the minimum outer rectangle of q_c to obtain the current line segment, which can be denoted by

$$(p_{q_c}^s, p_{q_c}^e) = rectangle(q_c),$$

$$l_{q_c} = (p_{q_c}^s, p_{q_c}^e).$$

This grouping strategy is applied over Q until all of its pixels are inactive. Denote the above procedures as $\phi = \{cente_align, group, rectangle\}$, the re-transformation function can be expressed as

$$\phi: G \xrightarrow{re-transforming} (\mathbb{R}^2, \mathbb{R}^2),$$

$$G \rightarrow \phi(G).$$

As a result, the line segments detected using the re-transformation function ϕ can be denoted by

$$C = \{l_{q_c} | q_c \in Q\}.$$

Parameterization We can parameterize the *center_align* model by searching the local observation window (e.g., $r_{w \times w}$, a $w \times w$ window is used) centred at q_c and finding more active pixels that are aligned with points of the current line segment with an angular distance less than a threshold (e.g., $\tau_d = 10^\circ$). Thus, we parameterize and rewrite *center_align* as

$$s = center_align(Q, q_c, c_c; r_{w \times w}, \tau_d).$$

To verify the candidate line segment, we can check the aspect ratio between the width and height of the approximated rectangle with respect to a predefined threshold (e.g., $r_{w/h}$) to ensure that the approximated rectangle is sufficiently thin. As a result, we parameterize and rewrite *rectangle* as

$$(p_{q_c}^s, p_{q_c}^e) = rectangle(q_c; r_{w/h}),$$

$$l_q = \begin{cases} null \\ Q_a = reactivate(Q_a, (q_c - q_0)) \\ (p_{q_c}^s, p_{q_c}^e) \end{cases} \quad \begin{matrix} if (p_{q_c}^s, p_{q_c}^e) == (null, null) \\ \\ otherwise \end{matrix},$$

in which if the verification fails, we keep q_0 inactive and reactivate $(q_c - q_0)$.

Generalization Encoder model: $\phi = \{cente_align, group, rectangle\}$; Input: $t = G$; Parameter: $\omega^e = \varepsilon = \{r_{w \times w}, \tau_d, r_{w/h}\}$; Output: $g = C$. Referring to Eq. (3), the encoder for the LSD task can be abbreviated as

$$C = encoder_{\{\phi\}}(G; \{\varepsilon\}). \quad (LSD-3)$$

(4) Learning

Referring to Eq. (4), in the learning procedure for the LSD task, we can empirically initialize the decoder with $\{\bar{\varphi}\}$ and utilize the initialized decoder to transform L labelled in an image lattice \mathcal{F} into a structured target by

$$\bar{E} = \text{decoder}_{\{R,a\}}(L; \{\bar{\varphi}\}). \quad (\text{LSD-4-1})$$

Then, we optimize the parameters of the inferrer by

$$\begin{aligned} \tilde{\theta} &= \arg \min_{\theta \in M^i} \frac{1}{N} \sum_{n=1}^N \ell^i \left(\text{inferred}(D_n; \{\theta\}), \bar{E} \right), \\ \ell^i \left(\text{inferred}(D; \{\theta\}), \bar{E} \right) &= \sum_{p \in \mathcal{F}} \|\bar{E}(p) - G(p)\|_1. \end{aligned} \quad (\text{LSD-4-2})$$

Then, we optimize the parameters of the encoder by

$$\begin{aligned} \tilde{\varepsilon} &= \arg \min_{\varepsilon \in M^e} \frac{1}{N} \sum_{n=1}^N \ell^e \left(\text{encoder}_{\{\phi\}}(C_n; \{\varepsilon\}), L_n \right), \\ \ell^e \left(\text{encoder}_{\{\phi\}}(C; \{\varepsilon\}), L \right) &= \frac{(C \cup L) - (C \cap L)}{C \cup L}. \end{aligned} \quad (\text{LSD-4-3})$$

(5) Looping

Usually, we loop several times to find relatively optimal parameters for the decoder. Referring to Eq. (5), the looping procedure for the LSD task can be defined as

$$\begin{aligned} \{\tilde{\varphi}\} &= \arg \min_{\{\varphi\} \in M^d} l(C|\{\varphi\}, L), \\ l(C|\{\varphi\}, L) &= \frac{((C|\{\varphi\}) \cup L) - ((C|\{\varphi\}) \cap L)}{(C|\{\varphi\}) \cup L}, \\ C|\{\varphi\} &= \text{encoder}_{\{\phi\}} \left(\text{inferred}(D; \{\tilde{\theta}\}); \{\tilde{\varepsilon}\} \right). \end{aligned} \quad (\text{LSD-5})$$

(6) Testing

Referring to Eq. (6), the testing procedure for the LSD task can be defined as

$$G = \text{inferred}_{\{\psi\}}(D; \{\tilde{\theta}\}|\{\tilde{\varphi}\}), \quad (\text{LSD-6-1})$$

$$C = \text{encoder}_{\{\phi\}}(G; \{\tilde{\varepsilon}\}|\{\tilde{\varphi}\}). \quad (\text{LSD-6-2})$$

4.3.3 Analysis

From the rebuilt solutions presented in section 4.3.1 and section 4.3.2 for the CD and LSD tasks, we draw a summarization as Fig. 8. From Fig. 8 we can note that the two solutions for the CD and LSD tasks can be abstractly expressed as the form of the MSL framework presented in section 4.2, though they have large differences in detailed implementations. In other words, by simply comparing the detailed implementations of the two solutions for CD and LSD, it is hard for one to instantly say that the two solutions intrinsically share the same methodological formation. However, by referring to the definition and framework presented for MSL, it is easy for one to say that the two solutions for CD and LSD intrinsically share the same methodological formation. This proves that generality exist in different MSL solutions, which have large differences, when we view them from an abstract point of view; that is, solutions for a wide variety of MSL tasks can probably be unified into the same abstract formation.

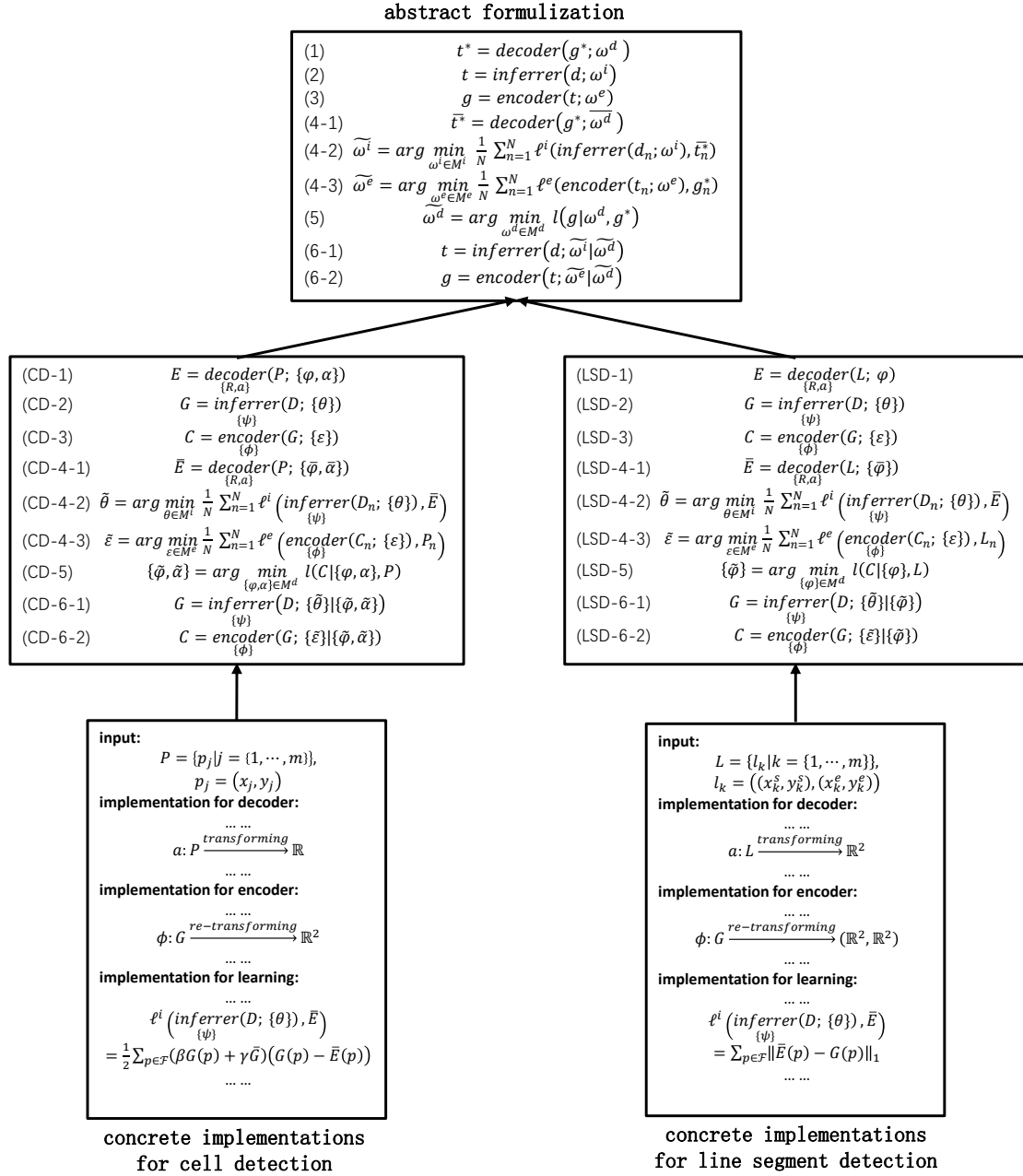


Fig. 8. Summarization of the rebuilt solutions for the CD and LSD tasks.

5. Discussion

In the current literature, by referring to the properties of the labels prepared for the training data set, learning with supervision is categorized as supervised learning (SL), which concerns the situation where the training data set is assigned with ideal (complete, exact and accurate) labels, and weakly supervised learning (WSL), which concerns the situation where the training data set is assigned with non-ideal (incomplete, inexact and inaccurate) labels. In this paper, we argue that the abstractness of the definition of the SL conceals some details that can be critical to building the appropriate solutions for certain specific SL tasks, noticing the given labels are not always learnable and the transformation from the given labels to learnable targets can significantly affect

the performance of the final SL solutions. Taking into consideration the properties of the transformation from the given labels to learnable targets, we categorize SL into three narrower sub-types including: precisely supervised learning (PSL), which concerns the situation where the given labels are precisely fine; moderately supervised learning (MSL), which concerns the situation where the given labels are ideal, but due to the simplicity in annotation of the given labels, careful designs are required to transform the given labels into learnable targets for the learning task; and precisely and moderately combined supervised learning (PMCSL) which concerns the situation where the given labels contain both precise and moderate annotations.

Due to the fact that the MSL subtype plays the central role in the field of SL, we comprehensively illustrate MSL from the perspectives of the definition, framework and generality to reveal what details are concealed by the abstractness of the definition of SL. Primarily, we present the definition of MSL which proves that some details are indeed concealed by the roughness of SL category. Subsequently, referring to the presented definition of MSL, we present the framework of MSL which reveals the key points of constructing fundamental MSL solutions and the key problems of developing better MSL solutions, which are critical to building the appropriate solutions but concealed by the abstractness of the definition of SL. Finally, analyses of the methodologies for two largely different MSL tasks (cell detection and line segment detection) prove that generality exist in different MSL solutions when we view them from an abstract point of view; that is, solutions for a wide variety of MSL tasks can probably be unified into the same abstract formation.

Specifically, the key points of constructing fundamental MSL solutions can be summarized as modelling three basic components including decoder, inferrer and encoder, and the key problems of developing better MSL solutions can be summarized as the learning and looping procedures to optimize the three basic components. The decoder, which is usually built and optimized on the basis of prior knowledge, is responsible for transforming the given labels into learnable targets. The inferrer, which is usually built and optimized on the basis of machine learning techniques, is responsible for mapping events/entities to corresponding learnable targets. The encoder, which is usually built and optimized on the basis of the decoder, is responsible for transforming the predicted targets of the inferrer into final predicted labels. While abundant modelling approaches [46–49] and optimization methods [50–52] have been proposed for the inferrer, the modelling and optimization of the decoder and the encoder lack systematic and comprehensive studies, except for some sporadic solutions for specific MSL tasks [3–6]. On one hand, although successful decoders [3–6] have been proposed for different MSL tasks, the general methodology for modelling an appropriate decoder for an MSL task is still unclear. As the decoder determines how an MSL task is defined and is the prerequisite for optimization of both the inferrer and decoder, it is valuable to investigate how to efficiently and effectively model a decoder for an MSL task with prior knowledge. On the other hand, because it is coupled with the decoder, small changes in the encoder can also significantly affect the final performance [3, 4, 53, 54]. Thus, it would also be interesting to investigate how to find an appropriate encoder for an MSL task. Respectively being the pre-processing and post-processing for the inferrer, the decoder and the encoder are both critical to building the appropriate solutions for MSL tasks, especially when the current state-of-the-art inferrer (deep neural networks from complex [8, 27–31] to lightweight [55–57]) has been becoming standardized and reaching its limits in many AI applications.

One significance of this paper is that, presenting the definition, framework and generality for

MSL, it provides the fundamental basis to systematically analyse the situation where the given labels are ideal, but due to the simplicity in annotation of the given labels, careful designs are required to transform the given labels into learnable targets. Moreover, taking into consideration the transformation from the given labels to learnable targets, it has been shown that SL tasks can be more concretely different in narrower subtypes though they share the same abstract definition of SL; and the illustrations for MSL have shown that the solutions for different MSL tasks can be unified into the same abstract formation though they have large differences in concrete implementations, which proves that a generality can probably exist among a wide variety of MSL tasks. Thus, the other significance of this paper is that it presents a tutorial for viewing a problem to be solved from the mathematicians' vision, which can be helpful for AI application engineers to discover, evaluate and select appropriate solutions for the problem to be solved.

Reference

1. LeCun Y, Bengio Y, Hinton G (2015) Deep learning. *Nature* 521:436–444. <https://doi.org/10.1038/nature14539>
2. Zhou Z-H (2018) A brief introduction to weakly supervised learning. *Natl Sci Rev* 5:44–53. <https://doi.org/10.1093/nsr/nwx106>
3. Xie Y, Xing F, Shi X, et al (2018) Efficient and robust cell detection: A structured regression approach. *Med Image Anal* 44:245–254. <https://doi.org/10.1016/j.media.2017.07.003>
4. Xue N, Bai S, Wang F-D, et al (2019) Learning Regional Attraction for Line Segment Detection. *IEEE Trans Pattern Anal Mach Intell.* <https://doi.org/10.1109/tpami.2019.2958642>
5. Lin TY, Dollár P, Girshick R, et al (2017) Feature pyramid networks for object detection. In: *Proceedings - 30th IEEE Conference on Computer Vision and Pattern Recognition, CVPR 2017*
6. Lin TY, Goyal P, Girshick R, et al (2020) Focal Loss for Dense Object Detection. *IEEE Trans Pattern Anal Mach Intell.* <https://doi.org/10.1109/TPAMI.2018.2858826>
7. Law H, Deng J (2020) CornerNet: Detecting Objects as Paired Keypoints. *Int J Comput Vis.* <https://doi.org/10.1007/s11263-019-01204-1>
8. Krizhevsky A, Sutskever I, Hinton GE (2012) ImageNet Classification with Deep Convolutional Neural Networks. In: *Advances in Neural Information Processing Systems*. pp 1097–1105
9. Ghosh S, Das N, Das I, Maulik U (2019) Understanding deep learning techniques for image segmentation. *ACM Comput Surv.* <https://doi.org/10.1145/3329784>
10. Zhao ZQ, Zheng P, Xu ST, Wu X (2019) Object Detection With Deep Learning: A Review. *IEEE Trans. Neural Networks Learn. Syst.*
11. Ranjan R, Patel VM, Chellappa R (2019) HyperFace: A Deep Multi-Task Learning Framework for Face Detection, Landmark Localization, Pose Estimation, and Gender Recognition. *IEEE Trans Pattern Anal Mach Intell.* <https://doi.org/10.1109/TPAMI.2017.2781233>
12. Cao Z, Hidalgo Martinez G, Simon T, et al (2019) OpenPose: Realtime Multi-Person 2D Pose Estimation using Part Affinity Fields. *IEEE Trans Pattern Anal Mach Intell.* <https://doi.org/10.1109/tpami.2019.2929257>
13. Zhang J (2016) Mathematicians' vision (in Chinese). Hubei Science and Technology Press,

Wuhan

14. Yang Y, Wu Y, Chen N (2019) Explorations on visual localization from active to passive. *Multimed Tools Appl* 78:2269–2309. <https://doi.org/10.1007/s11042-018-6347-0>
15. Yang Y, Chen N, Jiang S (2018) Collaborative strategy for visual object tracking. *Multimed Tools Appl* 77:7283–7303. <https://doi.org/10.1007/s11042-017-4633-x>
16. Yang Y, Lv H, Chen N, et al (2020) FTBME: feature transferring based multi-model ensemble. *Multimed Tools Appl* 79:18767–18799. <https://doi.org/10.1007/s11042-020-08746-4>
17. Yang Y, Lv H, Chen N, et al (2021) Local minima found in the subparameter space can be effective for ensembles of deep convolutional neural networks. *Pattern Recognit* 109:107582. <https://doi.org/10.1016/j.patcog.2020.107582>
18. Li F, Yang Y, Wei Y, et al (2021) Deep learning-based predictive biomarker of pathological complete response to neoadjuvant chemotherapy from histological images in breast cancer. *J Transl Med*. <https://doi.org/10.1186/s12967-021-03020-z>
19. Zhou ZH (2018) A brief introduction to weakly supervised learning. *Natl. Sci. Rev.*
20. Settles B (2010) Active Learning Literature Survey. *Mach Learn*. <https://doi.org/10.1.1.167.4245>
21. Zhu X (2008) Semi-Supervised Learning Literature Survey Contents. *Sci York*. <https://doi.org/10.1.1.146.2352>
22. Foulds J, Frank E (2010) A review of multi-instance learning assumptions. *Knowl. Eng. Rev.*
23. Frénay B, Verleysen M (2014) Classification in the presence of label noise: A survey. *IEEE Trans Neural Networks Learn Syst*. <https://doi.org/10.1109/TNNLS.2013.2292894>
24. Yang Y, Yang Y, Yuan Y, et al (2020) Detecting helicobacter pylori in whole slide images via weakly supervised multi-task learning. *Multimed Tools Appl* 79:26787–26815. <https://doi.org/10.1007/s11042-020-09185-x>
25. Yang Y, Yang Y, Chen J, et al (2020) Handling Noisy Labels via One-Step Abductive Multi-Target Learning: An Application to Helicobacter Pylori Segmentation
26. Yang Y (2021) One-Step Abductive Multi-Target Learning with Diverse Noisy Samples: An Application to Tumour Segmentation for Breast Cancer
27. Simonyan K, Zisserman A (2015) Very deep convolutional networks for large-scale image recognition. In: 3rd International Conference on Learning Representations, ICLR 2015 - Conference Track Proceedings
28. Szegedy C, Ioffe S, Vanhoucke V, Alemi AA (2017) Inception-v4, inception-ResNet and the impact of residual connections on learning. In: 31st AAAI Conference on Artificial Intelligence, AAAI 2017
29. He K, Zhang X, Ren S, Sun J (2016) Deep Residual Learning for Image Recognition. In: 2016 IEEE Conference on Computer Vision and Pattern Recognition (CVPR). IEEE, pp 770–778
30. Huang G, Liu Z, Maaten L van der, Weinberger KQ (2017) Densely Connected Convolutional Networks. In: 2017 IEEE Conference on Computer Vision and Pattern Recognition (CVPR). IEEE, pp 2261–2269
31. Hu J, Shen L, Sun G (2018) Squeeze-and-Excitation Networks. In: 2018 IEEE/CVF Conference on Computer Vision and Pattern Recognition. IEEE, pp 7132–7141
32. Redmon J, Divvala S, Girshick R, Farhadi A (2016) You only look once: Unified, real-time object detection. In: Proceedings of the IEEE Computer Society Conference on Computer Vision and Pattern Recognition

33. Redmon J, Farhadi A (2017) YOLO9000: Better, faster, stronger. In: Proceedings - 30th IEEE Conference on Computer Vision and Pattern Recognition, CVPR 2017
34. Redmon J, Farhadi A (2017) Yolov3. Proc IEEE Comput Soc Conf Comput Vis Pattern Recognit. <https://doi.org/10.1109/CVPR.2017.690>
35. Bochkovskiy A, Wang C-Y, Liao H-YM (2020) YOLOv4: Optimal Speed and Accuracy of Object Detection. arXiv.org
36. Liu W, Anguelov D, Erhan D, et al (2016) SSD: Single Shot MultiBox Detector. In: ECCV 2016
37. Girshick R, Donahue J, Darrell T, Malik J (2014) Rich feature hierarchies for accurate object detection and semantic segmentation. In: Proceedings of the IEEE Computer Society Conference on Computer Vision and Pattern Recognition
38. He K, Zhang X, Ren S, Sun J (2015) Spatial Pyramid Pooling in Deep Convolutional Networks for Visual Recognition. IEEE Trans Pattern Anal Mach Intell. <https://doi.org/10.1109/TPAMI.2015.2389824>
39. Girshick R (2015) Fast R-CNN. In: Proceedings of the IEEE International Conference on Computer Vision
40. Ren S, He K, Girshick R, Sun J (2017) Faster R-CNN: Towards Real-Time Object Detection with Region Proposal Networks. IEEE Trans Pattern Anal Mach Intell. <https://doi.org/10.1109/TPAMI.2016.2577031>
41. Sirinukunwattana K, Raza SEA, Tsang YW, et al (2016) Locality Sensitive Deep Learning for Detection and Classification of Nuclei in Routine Colon Cancer Histology Images. IEEE Trans Med Imaging. <https://doi.org/10.1109/TMI.2016.2525803>
42. Kainz P, Urschler M, Schultze S, et al (2015) You should use regression to detect Cells. In: Lecture Notes in Computer Science (including subseries Lecture Notes in Artificial Intelligence and Lecture Notes in Bioinformatics)
43. Matas J, Galambos C, Kittler J (2000) Robust detection of lines using the progressive probabilistic hough transform. Comput Vis Image Underst. <https://doi.org/10.1006/cviu.1999.0831>
44. Denis P, Elder JH, Estrada FJ (2008) Efficient edge-based methods for estimating manhattan frames in urban imagery. In: Lecture Notes in Computer Science (including subseries Lecture Notes in Artificial Intelligence and Lecture Notes in Bioinformatics)
45. von Gioi RG, Jakubowicz J, Morel J-M, Randall G (2010) LSD: A Fast Line Segment Detector with a False Detection Control. IEEE Trans Pattern Anal Mach Intell 32:722–732. <https://doi.org/10.1109/TPAMI.2008.300>
46. Shelhamer E, Long J, Darrell T (2017) Fully Convolutional Networks for Semantic Segmentation. IEEE Trans Pattern Anal Mach Intell 39:640–651. <https://doi.org/10.1109/TPAMI.2016.2572683>
47. Badrinarayanan V, Kendall A, Cipolla R (2017) SegNet: A Deep Convolutional Encoder-Decoder Architecture for Image Segmentation. IEEE Trans Pattern Anal Mach Intell 39:2481–2495. <https://doi.org/10.1109/TPAMI.2016.2644615>
48. Chen L-C, Papandreou G, Kokkinos I, et al (2018) DeepLab: Semantic Image Segmentation with Deep Convolutional Nets, Atrous Convolution, and Fully Connected CRFs. IEEE Trans Pattern Anal Mach Intell 40:834–848. <https://doi.org/10.1109/TPAMI.2017.2699184>
49. Falk T, Mai D, Bensch R, et al (2019) U-Net: deep learning for cell counting, detection, and morphometry. Nat Methods. <https://doi.org/10.1038/s41592-018-0261-2>

50. Bottou L (2010) Large-Scale Machine Learning with Stochastic Gradient Descent. In: Proceedings of COMPSTAT'2010
51. Duchi J, Hazan E, Singer Y (2011) Adaptive subgradient methods for online learning and stochastic optimization. J Mach Learn Res
52. Kingma DP, Ba JL (2015) Adam: A method for stochastic gradient descent. ICLR Int Conf Learn Represent
53. Bodla N, Singh B, Chellappa R, Davis LS (2017) Improving Object Detection With One Line of Code Navaneeth. Proc IEEE Int Conf Comput Vis. <https://doi.org/10.1109/ICCV.2017.593>
54. Hosang J, Benenson R, Schiele B (2017) Learning non-maximum suppression. In: Proceedings - 30th IEEE Conference on Computer Vision and Pattern Recognition, CVPR 2017
55. Howard A, Sandler M, Chen B, et al (2019) Searching for mobileNetV3. In: Proceedings of the IEEE International Conference on Computer Vision
56. Sun K, Li M, Liu D, Wang J (2019) IGCv3: Interleaved low-rank group convolutions for efficient deep neural networks. In: British Machine Vision Conference 2018, BMVC 2018
57. Zhang X, Zheng H, Sun J (2018) ShuffleNetV2. ECCV